Published in final edited form as:
Invest Radiol. 2010 October ; 45(10): 586–591. doi:10.1097/RLI.0b013e3181ed1b3b.

An Ultrasound Contrast Agent targeted to P-selectin detects Activated Platelets at Supra-arterial Shear Flow Conditions

Felix Guenther, MD[*], **Constantin von zur Muhlen, MD**[*], **Elisa A. Ferrante, PhD**[†,‡], **Sebastian Grundmann, MD, PhD**[*], **Christoph Bode, MD**[*], and **Alexander L. Klibanov, PhD**[†,‡,§,[//]]

[*]Department of Cardiology and Angiology, University Hospital of Freiburg, Freiburg, Germany

[†]Robert M. Berne Cardiovascular Research Center, University of Virginia, Charlottesville, VA

[‡]Division of Cardiovascular, Department of Medicine, University of Virginia School of Medicine, University of Virginia, Charlottesville, VA

[§]Department of Biomedical Engineering, University of Virginia, Charlottesville, VA

[[//]]Cardiovascular Imaging Center, University of Virginia, Charlottesville, VA

Abstract

Objectives—To evaluate targeting of a microbubble contrast agent to platelets under high shear flow using the natural selectin ligand sialyl Lewis[a].

Materials and Methods—Biotinylated polyacrylamide Sialyl Lewis[a] or biotinylated carbohydrate-free polymer (used as a control) were attached to biotinylated microbubbles via a streptavidin linker. Activated human platelets were isolated and attached to fibrinogen-coated culture dishes. Fibrinogen-coated dishes without platelets or platelet dishes blocked by an anti-P-selectin antibody served as negative control substrates. Dishes coated by recombinant P-selectin served as a positive control substrate. Microbubble adhesion was assessed by microscopy in an inverted parallel plate flow chamber, with wall shear stress values of 40, 30, 20, 10 and 5 dynes/cm^2. The ratio of binding and passing microbubbles was defined as capture efficiency.

Results—There was no significant difference between the groups regarding the number of microbubbles in the fluid flow at each shear rate. Sialyl Lewis[a]-targeted microbubbles were binding and slowly rolling on the surface of activated platelets and P-selectin-coated dishes at all the flow conditions including 40 dynes/cm^2. Capture efficiency of targeted microbubbles to activated platelets and recombinant P-selectin decreased with increasing shear flow: at 5 dynes/cm^2, capture efficiency was 16.11% on activated platelets vs. 21.83 % on P-selectin, and, at 40 dynes/cm^2, adhesion efficiency was still 3.4 % in both groups. There was neither significant adhesion of Sialyl Lewis[a]-targeted microbubbles to control substrates, nor adhesion of control microbubbles to activated platelets or to recombinant P-selectin.

Conclusions—Microbubble targeting using sialyl Lewis[a], a fast-binding ligand to P-selectin, is a promising strategy for the design of ultrasound contrast binding to activated platelets under high shear stress conditions.

Keywords

Ultrasound contrast; Targeted microbubbles; activated platelets; P-selectin; Sialyl Lewis[a]

Reprints: Felix Guenther, MD, Department of Cardiology and Angiology, University Hospital of Freiburg, Hugstetterstrasse 55, 79106 Freiburg, Germany. felix.guenther@uniklinik-freiburg.de.
Felix Guenther and Constantin von zur Muhlen contributed equally for this work.

Dr. A. Klibanov owns stock of Targeson, a startup company that manufactures microbubble contrast agents used in preclinical setting.

Introduction

Molecular imaging of atherosclerosis offers a promising approach to non-invasive detection and assessment of this disease. Activated platelets on the surface of ruptured, inflamed and unstable atherosclerotic plaques are of special interest[1,2]. The rupture of vulnerable atherosclerotic plaques is the critical event in thrombotic vessel occlusion in myocardial infarction[3]. However, platelets are also involved in earlier stages of plaque development. It has been revealed that platelets interact with activated endothelium before endothelial denudation and development of visible atherosclerotic lesions[2–4]. Advanced type atherosclerotic lesions with significant calcification and obstruction of the vessel lumen can be largely diagnosed by angiography or computer tomography. However, early stage atherosclerotic plaques, potentially associated with high vulnerability are generally asymptomatic ("silent plaques") and difficult to detect[5,6]. Hence, non-invasive imaging of vulnerable atherosclerotic plaques has been an attractive concept for a variety of imaging modalities, such as SPECT[7], PET[8] and MRI. In addition to the conventional imaging techniques using structural and geometric determinants or unspecific iron uptake of macrophages[9,10], there are also molecular imaging techniques that become an important component in the diagnosis of vulnerable plaques. In this setting, the contrast agents are linked to chosen ligands which selectively bind to molecules expressed on the plaque surface, like the activated GP IIb/IIIa receptor[11], the scavenger receptor of macrophages[12], or other molecules expressed by extracellular matrix, thrombi and neovasculature[13–21]. Thus, molecular ultrasound imaging of aggregated or adhering platelets may also offer a non-invasive diagnostic tool to identify thrombi within unstable atherosclerotic plaques.

The large size of the ultrasound contrast microbubbles (typically ~2–4 μm in diameter) combined with the slow association kinetic properties of many targeting ligands, e.g. antibodies[22], have been a problem concerning firm adhesion under high shear flow. Under these conditions, targeting ligands on the bubble surface may not have sufficient time to attach to the receptor, so microbubble binding is inefficient[23–26]. Several strategies have been considered to improve microbubble capture efficiency on the target of interest: acoustic radiation force which concentrates and decelerates the microbubbles near the vessel wall[27], deformable microbubbles with high contact area to target surface[28], or the use of fast binding molecules as selectin ligands from the sialyl Lewis group[23,25,26]. These selectin ligands are characterized by a high on-rate and off-rate and are identified as mediators of leukocyte rolling and adhesion to P- and E-selectins on the inflamed endothelium under high shear flow in vivo[23,25,26,29–31]. Platelet activation leads to P-selectin expression on the membrane in an amount of about 12000 molecules per platelet[32,33]. Normal arterial wall shear stress ranges from ~10 to ~40 dynes/cm^2 [34,35]. In previously released studies on platelet targeting, microbubbles were carrying ligands against the glycoprotein IIb-IIIa complex. These adhesion experiments were either performed under static conditions or did not exceed 5 dynes/cm^2 under dynamic flow conditions[36–38]. The aim of our study was to evaluate microbubble platelet targeting with a contrast agent that binds under high shear flow conditions up to 40 dynes/cm^2 using the selectin ligand sialyl Lewis^a (sLe^a) as the targeting molecule.

Material and Methods

Preparation of microbubbles

Microbubbles (MB) were prepared according to established procedures[39]. Briefly, MB had decafluorobutane gas core encapsulated by a phosphatidylcholine lipid monolayer shell. A brush of polyethylene glycol (PEG) was attached onto the lipid shell via a lipid anchor

embedded in the lipid monolayer. Some of the PEG molecules contained biotin at the distal tip[39]. Targeting was achieved by coupling biotinylated sLe^a ligand (Sialyl $Lewis^a$-polyacrylamide-biotin, Glycotech, Gaithersburg, Maryland, USA) to the biotinylated MB via a streptavidin linker (figure 1). Biotinylated MB were washed with degassed phosphate buffered saline (Dulbecco's PBS, Sigma, St. Louis, Missouri, USA) by centrifugation (400 × g for 3 min) to remove excess free unincorporated lipid, and incubated with streptavidin (Sigma, St. Louis, Missouri, USA) for 10 minutes at room temperature (3 μg streptavidin per 10^7 MB). Excess streptavidin was removed by centrifugation and elimination of the infranatant. After that, MB were incubated either with biotinylated sLe^a ligand or with a biotinylated control polyacrylamide (control-PAA) with the same backbone without carrying the functional sialyl Lewis groups ($HOCH_2(HOCH)_4CH_2NH$-PAA-biotin, Glycotech, Gaithersburg, Maryland, USA) for 10 minutes at room temperature (1.5 μg sLe^a ligand or control-PAA per 10^7 MB). MB were washed again to remove unreacted ligand and stored at 4°C. MB size distribution was determined by microscopy observations. MB concentration was assessed with a hemocytometer. Aggregation of MB as the result of ligand coupling procedure was minimal. Mean MB size was 2.71 μm (± 0.05 μm SEM).

Preparation of platelet concentrate

Blood from healthy volunteers taking no medication was anti-coagulated with citric acid and centrifuged at 150 × g for ten minutes. The resulting platelet-rich plasma was separated and recentrifuged at 2000 × g for 10 minutes. The resulting platelet pellet was then separated from the platelet-poor plasma. The platelets were resuspended in PBS in a concentration of about 250000 platelets/ml. For platelet activation, adenosine diphosphate (ADP, möLab, Langenfeld, Germany) was added immediately prior to platelet incubation on the dishes (20 μM final concentration, see also next section).

Target preparation for flow-chamber adhesion studies

For the flow chamber adhesion studies, polystyrene culture dishes (35mm, Corning, New York, USA) were coated with recombinant P-selectin or activated platelets on a fibrinogen layer. As negative control, fibrinogen-coated dishes without platelets and platelet-coated dishes pre-incubated with an anti-P-selectin antibody (R&D Systems, Minneapolis, Minnesota, USA) were prepared. The antibody was used in order to block the sLe^a-binding sites on the platelets to demonstrate the specific binding of sLe^a-targeted microbubbles (sLe^a MB) to P-selectin. Dishes were incubated with droplets of either 200 μl of recombinant P-selectin (9 μg/ml in PBS, R&D Systems) or 200 μl of fibrinogen (100 μg/ml in PBS, Enzyme Research Laboratories, Swansea, UK) which were placed in the center of the dish and sheltered by a plastic cover slip to provide uniform protein coverage and to avoid evaporation of the solution. Incubation was overnight at 4 °C in a chamber with high humidity. The dishes were washed with PBS three times and blocked with 2 ml of blocker casein solution in TBS (Pierce, Rockford, Illinois, USA) for at least 2 hours at 4 °C. Blocked dishes were washed excessively with PBS. P-selectin and pure fibrinogen dishes were now ready for experiments. Platelet coverage was achieved by incubating the fibrinogen-coated dishes with 1 ml of ADP-activated human platelet medium for 30 min at 37 °C. The ADP was added to the platelets immediately prior to incubation on the dishes (20 μM final concentration). A uniform and dense coverage of activated platelets on the dish without formation of platelet aggregates was achieved, as observed by microscopy (40 fold objective magnification). The dishes were washed again with PBS for several times. As negative control, platelet dishes were incubated with an anti-P-selectin antibody for 30 minutes at 37 °C (100 μg antibody in 1 ml PBS, R&D Systems, Minneapolis, USA). The dishes were washed three times with PBS to remove free unreacted antibody.

Flow-chamber adhesion efficiency experiments

A parallel plate flow chamber system was used to characterize microbubble adhesion efficiency to substrates[22,39] absorbed with recombinant P-selectin, activated platelets, fibrinogen, and activated platelets pre-incubated with an anti-P-selectin antibody. A silicon gasket attached to a flow deck by vacuum grease defined a rectangular flow path with a width of 2.5 mm, height of 0.127 mm and a length of 20 mm (Gasket A, Glycotech, Gaithersburg, Maryland, USA). The wall shear stress within the chamber was determined according to the following equation: $\tau = \frac{6\mu Q}{bh^2}$, where τ denotes wall shear stress (in N/m^2), μ is the fluid viscosity (0.001 N/s^2 for water at 20 °C), Q is the fluid flow rate (m^3/s), b is the chamber width (m), and h is the chamber height (m). Wall shear stress was calculated in dynes/cm^2 (1 dyne/cm^2 = 1 μ bar = 0.1 Pa). The flow chamber was placed in a custom built mount, which inverted the flow deck to account for MB buoyancy. The chamber was sealed using a plastic screw with an o-ring lubricated with vacuum grease. The vacuum port on the flow deck was sealed with a dead-end tube fitting[39]. Two pieces of polyethylene tubing (Intramedic PE 60 Tubing, BD Sciences, Franklin Lakes, New Jersey, USA) were cut to a length of about 15 cm and inserted in the 2 polypropylene tubing connectors located at the bottom of the flow deck. One tube was connected to the vial with MB dispersion, the second tube was connected to a three-way stopcock with two 10 ml syringes placed orthogonally to each other (BD Sciences, Franklin Lakes, New Jersey, USA). One syringe was fixed in a syringe pump (Harvard Apparatus, Holliston, Massachusetts, USA) to create shear flow by withdrawing the plunger and to collect medium waste. The other syringe contained PBS with calcium and magnesium (Dulbecco's PBS, Sigma, St. Louis, Missouri, USA). For the experiments, a MB dispersion with sLe^a-targeted or control MB in 6 ml PBS with calcium and magnesium (5×10^6 MB/ml PBS) was prepared in a plastic test-tube and mixed continuously by a magnetic stirrer. BSA (0.4%) was added to PBS to block unspecific binding sites during the experiment. A culture dish with the target was then fixed in the flow chamber and the system was vented completely. The center of the flow chamber was monitored by microscopy. A microscope CCD-camera (Horn, Aalen, Germany) that was connected to a PC with capture software (Let's Edit RT Version 1.01, Canopus Co. Ltd, Grass Valley, San Jose, California, USA) transferred real time pictures to PC for recording (field of view 420 × 350 μm). The syringe pump operated in the withdrawal mode to generate wall shear stress of 40, 30, 20, 10 and 5 dynes/cm^2, respectively. The required refill rate of the syringe pump was calculated according to the equation above. After a short delay necessary for the stabilization of the microbubble flux, a 60 second time period video was digitally recorded at each shear stress with a frame rate of 25 Hz. Each dish was exposed once to each shear rate, beginning at the highest shear rate of 40 dynes/cm^2 and terminating with 5 dynes/cm^2. Different microbubble groups and dish substrates are summarized in table 1. Attaching and passing MB were counted in the field of view. The ratio of binding and passing MB (MB in the field of view that did not adhere to the surface) was defined as capture efficiency. SLe^a MB were tested on the recombinant P-selectin surface (4 dishes), activated platelets on fibrinogen (5 dishes), fibrinogen alone (3 dishes) and on the surface of activated platelets that had been pre-incubated with an anti P-selectin antibody (2 dishes). Control-PAA MB were tested on P-selectin surface (3 dishes) and activated platelets on fibrinogen (3 dishes).

Statistical analysis

Data were expressed as mean ± standard error of the mean (SEM). Statistical analysis was performed by an ANOVA test with Bonferroni correction. A p-value < 0.05 was considered to be statistically significant.

Results

Microbubble flux

The quantity of microbubbles in the flow is shown in table 1 (mean MB flux). The mean MB flux of each group (± SEM) is shown in table 1. Microbubble flux was determined by counting the passing microbubbles. Overall, the number of passing microbubbles ranged between 572/min (sLe^a MB on platelets, 5 dynes/cm^2) to 1454/min (sLe^a MB on platelets blocked by anti-P-selectin antibody, 40 dynes/cm^2).

At each wall shear stress, there was no significant difference between the different groups regarding microbubble flux. Within one group, we compared the microbubble flux at each shear rate with the flux at all the other shear rates: in each group, mean MB flux was increasing with higher shear stress, but this gradual increase was not statistically significant. In the group of sLe^a MB on platelet dishes that had been pre-incubated with an anti-P-selectin antibody, there were no significant differences of the numbers of passing MB between the different shear rates. In the other groups, MB flux at 40 dynes/cm^2 was significantly higher than the flux at 5 dynes/cm^2. In the group of sLea MB on fibrinogen without platelets, the differences between the flux at 5 and 30 dynes/cm^2 and the flux at 10 and 40 dynes/cm^2 were also statistically significant.

SLe^a MB on platelets and on recombinant P-selectin

SLe^a MB were attaching to the platelets and to recombinant P-selectin at all tested flow conditions. After initial adhesion, sLe^a MB were slowly rolling on the surface of platelets and of recombinant P-selectin along the flow path, caused by continual detachment (due to drag forces created by the fluid flow) and quick re-attachment of sLe^a to P-selectin. Under static conditions, when shear flow application was interrupted, adhesive sLe^a MB stopped rolling and maintained in their current position (figure 3). Capture efficiency was decreasing with increasing wall shear stress (table 1, figure 4). Capture efficiency of sLe^a MB on platelets and on recombinant P-selectin was in a comparable range and only significantly different at a wall shear stress of 5 dynes/cm^2, where MB adhesion was 21.84% (± 1.65 SEM) on recombinant P-selectin versus 16.11% (± 0.58 SEM) on platelets. At the fastest flow studied, 40 dynes/cm^2, there was still capture of sLe^a MB observed: 3.42% (± 0.1 SEM) on recombinant P-selectin and 3.39 (± 0.2 SEM) on activated platelets.

SLe^a MB on control dishes

There was only minimal and no significant binding of sLe^a MB on activated platelets pre-treated by an anti-P-selectin antibody at 5 and 10 dynes/cm^2, and these MB were detaching again immediately after adhesion (< 0.5 seconds) without re-attachment. At any shear flow from 5 to 40 dynes/cm^2, sLe^a MB did not bind on fibrinogen-coated dishes without platelets.

Control MB on activated platelets and on recombinant P-selectin

Control-PAA MB did not adhere either to activated platelets, or to recombinant P-selectin surface. Thus, capture efficiency of control and sLe^a-targeted MB was significantly different (see also table 1).

Discussion

In this study we have for the first time demonstrated specific binding of targeted microbubbles to P-selectin on the surface of activated platelets at fast flow conditions, up to 40 dynes/cm^2 shear stress. We observed decreased capture efficiency of sLe^a MB on activated platelets and on recombinant P-selectin with increasing shear flow. At maximum shear flow of 40 dynes/cm^2, we still detected a significant adhesion of sLe^a MB to the target.

Selectin ligand sialyl Lewis^a was applied for MB targeting in this study. SLe^a is chemically identical with the cancer antigen 19–9 and a growing body of knowledge suggests that this molecule plays an important role in the formation of metastases by colon and pancreatic cancer cells[40,41]. SLe^a is known for a very high on-rate and off-rate of selectin binding, unlike e.g., many antibody ligands. In vivo, sialyl Lewis-based ligands mediate leukocyte adhesion and rolling on endothelium[30,42–48]. In our experimental setting, targeted microbubbles were mimicking leukocytes in-vivo: after adhesion, sLe^a MB were slowly rolling on the surface of platelets or recombinant P-selectin in the flow direction. This can be explained by the experimental conditions and the kinetic properties of sLe^a. After MB adhesion under high shear flow takes place, the adherent MB are still exposed to the viscous drag forces as a result of the fluid flow. SLe^a MB can dissociate from their P-selectin targets due to these drag forces. If the density of the P-selectin molecules on the target surface is sufficiently high, microbubble translation and fast re-attachment to the surface-bound P-selectin molecules located downstream occurs, and MB rolling takes place. If the target selectin molecules density is low, the MB detach without a chance to re-attach and rapidly move out with the flow. We created a high P-selectin surface density condition by homogeneous coating of platelet dishes or by using a saturating P-selectin concentration on recombinant P-selectin dishes, with a resulting density of about 800 P-selectin molecules/ μm^2 [39].

Biotinylated polyacrylamide with the same degree of polymerization as PAA-sLe^a was linked to MB as a negative control. Under high shear flow, control microbubbles did not adhere either to platelets or to recombinant P-selectin. A few control MB adhered under static conditions before shear flow was applied. Under high shear flow conditions, however, these MB were not rolling on the surface or they detached rapidly. SLe^a MB did not stick either to fibrinogen without platelets or to platelets which had been incubated with an anti-P-selectin antibody before. The adherence of a small number of sLe^a MB on pre-treated platelet dishes at 5 and 10 dynes/cm^2 was significantly lower than on regular platelet dishes and these MB detached immediately after adhesion. This short-term attachment is most probably explainable by incomplete blocking by the antibody. These results confirm the specificity of the binding of sLe^a MB towards P-selectin and not to other binding sites on platelets, fibrinogen or the dish surface, respectively.

Possible indications for the application of the described contrast agent involve inflamed endothelium and vulnerable atherosclerotic plaques. During the development of atherosclerotic lesions, the endothelium becomes activated and adhesion molecules like VCAM1, ICAM1 and selectins are expressed, which are characteristic for inflamed endothelium. This results in the recruitment of white blood cells, which triggers and maintains vessel wall inflammation with lipid deposition, calcification, extracellular matrix digestion, apoptosis, smooth muscle cell proliferation and thrombosis. There are several morphologic and biologic criteria of plaque vulnerability, such as platelet aggregation [49,50]. In vivo, P-selectin is expressed by activated platelets and by activated endothelium[31]. Therefore, sLe^a MB would adhere not only to activated platelets but also to inflamed endothelium at early stages of plaque development. However, regardless of reduced target specificity, at early stages of atherosclerosis, MB should be able to visualize both activated endothelium and activated platelets.

MB rolling may become a problem relating to ultrasound assessment of atherosclerosis: after adhesion, MB roll on the target P-selectin molecules along the blood flow direction. As soon as the plaque ends and no more P-selectin molecules are present, MB will detach and transport out of the target area by the blood flow.

These problems might be solved by dual targeting approach. In this concept, a microbubble will be decorated with two different ligands, a fast-binding ligand such as sLe^a and a firm-binding ligand such as an antibody or a peptide that binds to another platelet surface molecule, e.g., the GPIIb/IIIa receptor. After the fast binding ligand on the microbubble has captured under high shear flow, there should be sufficient time for the second ligand to generate a specific and strong bond to anchor the microbubble on the target[39,51]. Alternatively, increasing the ligand density on the microbubble surface (e.g., by using covalently attached sLe^a on the microbubble shell) may improve its resistance to movement in high-shear flow[52], so that instead of rolling, firm adhesion of microbubbles to P-selectin targets may become possible.

Limitations

In this study, we demonstrated specific adhesion of targeted MB to P-selectin on activated platelets by microscopy in a model flow chamber system. For further evaluation of the usefulness of this system for targeted ultrasound imaging of activated platelets, in vitro and in vivo targeted ultrasound contrast studies need to be performed.

At 40, 30, 20 and 10 dynes/cm^2, there was no significant difference between capture efficiency of sLea MB on platelets and on recombinant P-selectin. At 5 dynes/cm^2, however, the adhesion of sLe^a MB to recombinant P-selectin was significantly above the adhesion of MB to platelets (21.84% vs. 16.11%, $p<0.05$). Several factors may have affected the capture probability: the effective wall shear stress, the density of target molecules, the configuration of the target surface and the properties of the fluid flow. Immobilized platelets on the dish extend into the flow channel, and thus, the 'real' channel height is less than the original gasket height: according to a mean platelet diameter of 3 μm[33], the effective wall shear stress is about 5% higher on platelet dishes than on dishes without corpuscular parts. Preliminary tests revealed that our P-selectin plating concentration of 9 μg/ml PBS leads to a P-selectin saturation with a density of about 800 molecules/μm^2 [39]. Assuming a platelet surface area of 12 μm^2 (in activated state) and a number of 12000 P-selectin molecules per activated platelet[33], the mean P-selectin density on an ideal platelet dish would be 1000 molecules/μm^2. However, even if the platelet coverage is dense, there are small gaps between directly adjacent platelets, so overall density might be lower than 1000 molecules/cm^2. In this study, we did not determine the mean P-selectin density on platelet dishes. Furthermore, we did not examine the influence of the platelets on the properties of the dish surface and fluid flow.

Conclusions

In conclusion, targeting of microbubbles using fast binding selectin ligands like sialyl $Lewis^a$ is a promising and effective strategy for the design of ultrasound contrast agents that bind to activated platelets under fast flow. These results encourage further in-vivo studies.

Acknowledgments

Supported by grants of the German Research Foundation (Dr. von zur Mehlen, No. MU2727/3-1) and the NIH (Dr. Klibanov, No. R21/33CA102880 and No. R01EB002185).

This study was supported by grants of the German Research Foundation (Dr. von zur Muhlen, grant-no MU2727/3-1) and the NIH (Dr. Klibanov, grant-no R21/33CA102880 and R01EB002185). The technical assistance of Irene Neudorfer as well as fruitful discussions with J. Rychak (Targeson) are greatly appreciated.

References

1. von zur Muhlen C, von Elverfeldt D, Moeller JA, et al. Magnetic resonance imaging contrast agent targeted toward activated platelets allows in vivo detection of thrombosis and monitoring of thrombolysis. Circulation. 2008; 118:258–267. [PubMed: 18574047]
2. Massberg S, Brand K, Gruner S, et al. A critical role of platelet adhesion in the initiation of atherosclerotic lesion formation. J Exp Med. 2002; 196:887–896. [PubMed: 12370251]
3. Corti R, Farkouh ME, Badimon JJ. The vulnerable plaque and acute coronary syndromes. Am J Med. 2002; 113:668–680. [PubMed: 12505118]
4. Gawaz M, Langer H, May AE. Platelets in inflammation and atherogenesis. J Clin Invest. 2005; 115:3378–3384. [PubMed: 16322783]
5. Stary HC, Chandler AB, Dinsmore RE, et al. A definition of advanced types of atherosclerotic lesions and a histological classification of atherosclerosis. A report from the Committee on Vascular Lesions of the Council on Arteriosclerosis, American Heart Association. Arterioscler Thromb Vasc Biol. 1995; 15:1512–1531. [PubMed: 7670967]
6. Matter CM, Stuber M, Nahrendorf M. Imaging of the unstable plaque: how far have we got? Eur Heart J. 2009; 30:2566–2574. [PubMed: 19833636]
7. Langer HF, Haubner R, Pichler BJ, et al. Radionuclide imaging: a molecular key to the atherosclerotic plaque. J Am Coll Cardiol. 2008; 52:1–12. [PubMed: 18582628]
8. Skajaa T, Cormode DP, Falk E, et al. High-Density Lipoprotein-Based Contrast Agents for Multimodal Imaging of Atherosclerosis. Arterioscler Thromb Vasc Biol. 2009
9. Corot C, Petry KG, Trivedi R, et al. Macrophage imaging in central nervous system and in carotid atherosclerotic plaque using ultrasmall superparamagnetic iron oxide in magnetic resonance imaging. Invest Radiol. 2004; 39:619–625. [PubMed: 15377941]
10. Li ZY, Tang TJUK-I, et al. Assessment of carotid plaque vulnerability using structural and geometrical determinants. Circ J. 2008; 72:1092–1099. [PubMed: 18577817]
11. von Zur Muhlen C, von Elverfeldt D, Choudhury RP, et al. Functionalized magnetic resonance contrast agent selectively binds to glycoprotein IIb/IIIa on activated human platelets under flow conditions and is detectable at clinically relevant field strengths. Mol Imaging. 2008; 7:59–67. [PubMed: 18706288]
12. Amirbekian V, Lipinski MJ, Briley-Saebo KC, et al. Detecting and assessing macrophages in vivo to evaluate atherosclerosis noninvasively using molecular MRI. Proc Natl Acad Sci U S A. 2007; 104:961–966. [PubMed: 17215360]
13. Briley-Saebo KC, Mulder WJ, Mani V, et al. Magnetic resonance imaging of vulnerable atherosclerotic plaques: current imaging strategies and molecular imaging probes. J Magn Reson Imaging. 2007; 26:460–479. [PubMed: 17729343]
14. Burgstahler C, Hombach V, Rasche V. Molecular imaging of vulnerable plaque by cardiac magnetic resonance imaging. Semin Thromb Hemost. 2007; 33:165–172. [PubMed: 17340465]
15. Burtea C, Laurent S, Murariu O, et al. Molecular imaging of alpha v beta3 integrin expression in atherosclerotic plaques with a mimetic of RGD peptide grafted to Gd-DTPA. Cardiovasc Res. 2008; 78:148–157. [PubMed: 18174291]
16. Burtea C, Laurent S, Port M, et al. Magnetic resonance molecular imaging of vascular cell adhesion molecule-1 expression in inflammatory lesions using a peptide-vectorized paramagnetic imaging probe. J Med Chem. 2009; 52:4725–4742. [PubMed: 19580288]
17. Flacke S, Fischer S, Scott MJ, et al. Novel MRI contrast agent for molecular imaging of fibrin: implications for detecting vulnerable plaques. Circulation. 2001; 104:1280–1285. [PubMed: 11551880]
18. Laufer EM, Winkens MH, Narula J, et al. Molecular imaging of macrophage cell death for the assessment of plaque vulnerability. Arterioscler Thromb Vasc Biol. 2009; 29:1031–1038. [PubMed: 19461053]
19. Vymazal J, Spuentrup E, Cardenas-Molina G, et al. Thrombus imaging with fibrin-specific gadolinium-based MR contrast agent EP-2104R: results of a phase II clinical study of feasibility. Invest Radiol. 2009; 44:697–704. [PubMed: 19809344]

20. Wilensky RL, Song HK, Ferrari VA. Role of magnetic resonance and intravascular magnetic resonance in the detection of vulnerable plaques. J Am Coll Cardiol. 2006; 47:C48–56. [PubMed: 16631510]
21. Zheng J, Ochoa E, Misselwitz B, et al. Targeted contrast agent helps to monitor advanced plaque during progression: a magnetic resonance imaging study in rabbits. Invest Radiol. 2008; 43:49–55. [PubMed: 18097277]
22. Takalkar AM, Klibanov AL, Rychak JJ, et al. Binding and detachment dynamics of microbubbles targeted to P-selectin under controlled shear flow. J Control Release. 2004; 96:473–482. [PubMed: 15120903]
23. Klibanov AL. Ultrasound molecular imaging with targeted microbubble contrast agents. J Nucl Cardiol. 2007; 14:876–884. [PubMed: 18022115]
24. Klibanov AL, Rychak JJ, Yang WC, et al. Targeted ultrasound contrast agent for molecular imaging of inflammation in high-shear flow. Contrast Media Mol Imaging. 2006; 1:259–266. [PubMed: 17191766]
25. Rychak JJ, Li B, Acton ST, et al. Selectin ligands promote ultrasound contrast agent adhesion under shear flow. Mol Pharm. 2006; 3:516–524. [PubMed: 17009850]
26. Klibanov AL. Microbubble contrast agents: targeted ultrasound imaging and ultrasound-assisted drug-delivery applications. Invest Radiol. 2006; 41:354–362. [PubMed: 16481920]
27. Dayton P, Klibanov A, Brandenburger G, et al. Acoustic radiation force in vivo: a mechanism to assist targeting of microbubbles. Ultrasound Med Biol. 1999; 25:1195–1201. [PubMed: 10576262]
28. Rychak JJ, Lindner JR, Ley K, et al. Deformable gas-filled microbubbles targeted to P-selectin. J Control Release. 2006; 114:288–299. [PubMed: 16887229]
29. Kobzdej MM, Leppanen A, Ramachandran V, et al. Discordant expression of selectin ligands and sialyl Lewis x-related epitopes on murine myeloid cells. Blood. 2002; 100:4485–4494. [PubMed: 12393554]
30. Ley K. Molecular mechanisms of leukocyte recruitment in the inflammatory process. Cardiovasc Res. 1996; 32:733–742. [PubMed: 8915191]
31. McEver RP. Role of selectins in leukocyte adhesion to platelets and endothelium. Ann N Y Acad Sci. 1994; 714:185–189. [PubMed: 7517114]
32. Gawaz M, Neumann FJ, Schomig A. Evaluation of platelet membrane glycoproteins in coronary artery disease: consequences for diagnosis and therapy. Circulation. 1999; 99:E1–E11. [PubMed: 9884400]
33. White, J. Anatomy and structural organization of the platelet. 2. Philadelphia: JB Lippincozz Co; 1994.
34. Stehbens WE. The role of hemodynamics in the pathogenesis of atherosclerosis. Prog Cardiovasc Dis. 1975; 18:89–103. [PubMed: 1098111]
35. Zarins CK, Bomberger RA, Glagov S. Local effects of stenoses: increased flow velocity inhibits atherogenesis. Circulation. 1981; 64:II221–227. [PubMed: 7249326]
36. Alonso A, Della Martina A, Stroick M, et al. Molecular imaging of human thrombus with novel abciximab immunobubbles and ultrasound. Stroke. 2007; 38:1508–1514. [PubMed: 17379828]
37. Martin MJ, Chung EM, Goodall AH, et al. Enhanced detection of thromboemboli with the use of targeted microbubbles. Stroke. 2007; 38:2726–2732. [PubMed: 17823379]
38. Schumann PA, Christiansen JP, Quigley RM, et al. Targeted-microbubble binding selectively to GPIIb IIIa receptors of platelet thrombi. Invest Radiol. 2002; 37:587–593. [PubMed: 12393970]
39. Ferrante EA, Pickard JE, Rychak J, et al. Dual targeting improves microbubble contrast agent adhesion to VCAM-1 and P-selectin under flow. J Control Release. 2009; 140:100–107. [PubMed: 19666063]
40. Sakamoto S, Watanabe T, Tokumaru T, et al. Expression of Lewisa, Lewisb, Lewisx, Lewisy, siayl-Lewisa, and sialyl-Lewisx blood group antigens in human gastric carcinoma and in normal gastric tissue. Cancer Res. 1989; 49:745–752. [PubMed: 2910493]
41. Ugorski M, Laskowska A. Sialyl Lewis(a): a tumor-associated carbohydrate antigen involved in adhesion and metastatic potential of cancer cells. Acta Biochim Pol. 2002; 49:303–311. [PubMed: 12362971]

42. Green PJ, Tamatani T, Watanabe T, et al. High affinity binding of the leucocyte adhesion molecule L-selectin to 3′-sulphated-Le(a) and -Le(x) oligosaccharides and the predominance of sulphate in this interaction demonstrated by binding studies with a series of lipid-linked oligosaccharides. Biochem Biophys Res Commun. 1992; 188:244–251. [PubMed: 1384480]
43. Greenberg AW, Brunk DK, Hammer DA. Cell-free rolling mediated by L-selectin and sialyl Lewis(x) reveals the shear threshold effect. Biophys J. 2000; 79:2391–2402. [PubMed: 11053118]
44. Nelson RM, Dolich S, Aruffo A, et al. Higher-affinity oligosaccharide ligands for E-selectin. J Clin Invest. 1993; 91:1157–1166. [PubMed: 7680663]
45. Revelle BM, Scott D, Kogan TP, et al. Structure-function analysis of P-selectin-sialyl LewisX binding interactions. Mutagenic alteration of ligand binding specificity. J Biol Chem. 1996; 271:4289–4297. [PubMed: 8626776]
46. Varki A. Selectin ligands. Proc Natl Acad Sci U S A. 1994; 91:7390–7397. [PubMed: 7519775]
47. Weitz-Schmidt G, Stokmaier D, Scheel G, et al. An E-selectin binding assay based on a polyacrylamide-type glycoconjugate. Anal Biochem. 1996; 238:184–190. [PubMed: 8660609]
48. Zhang X, Bogorin DF, Moy VT. Molecular basis of the dynamic strength of the sialyl Lewis X-selectin interaction. Chemphyschem. 2004; 5:175–182. [PubMed: 15038277]
49. Sanz J, Fayad ZA. Imaging of atherosclerotic cardiovascular disease. Nature. 2008; 451:953–957. [PubMed: 18288186]
50. Wu JC, Bengel FM, Gambhir SS. Cardiovascular molecular imaging. Radiology. 2007; 244:337–355. [PubMed: 17592037]
51. Weller GE, Villanueva FS, Tom EM, et al. Targeted ultrasound contrast agents: in vitro assessment of endothelial dysfunction and multi-targeting to ICAM-1 and sialyl. Lewisx Biotechnol Bioeng. 2005; 92:780–788.
52. Klibanov AL, Hughes MS, Villanueva FS, et al. Targeting and ultrasound imaging of microbubble-based contrast agents. MAGMA. 1999; 8:177–184. [PubMed: 10504045]

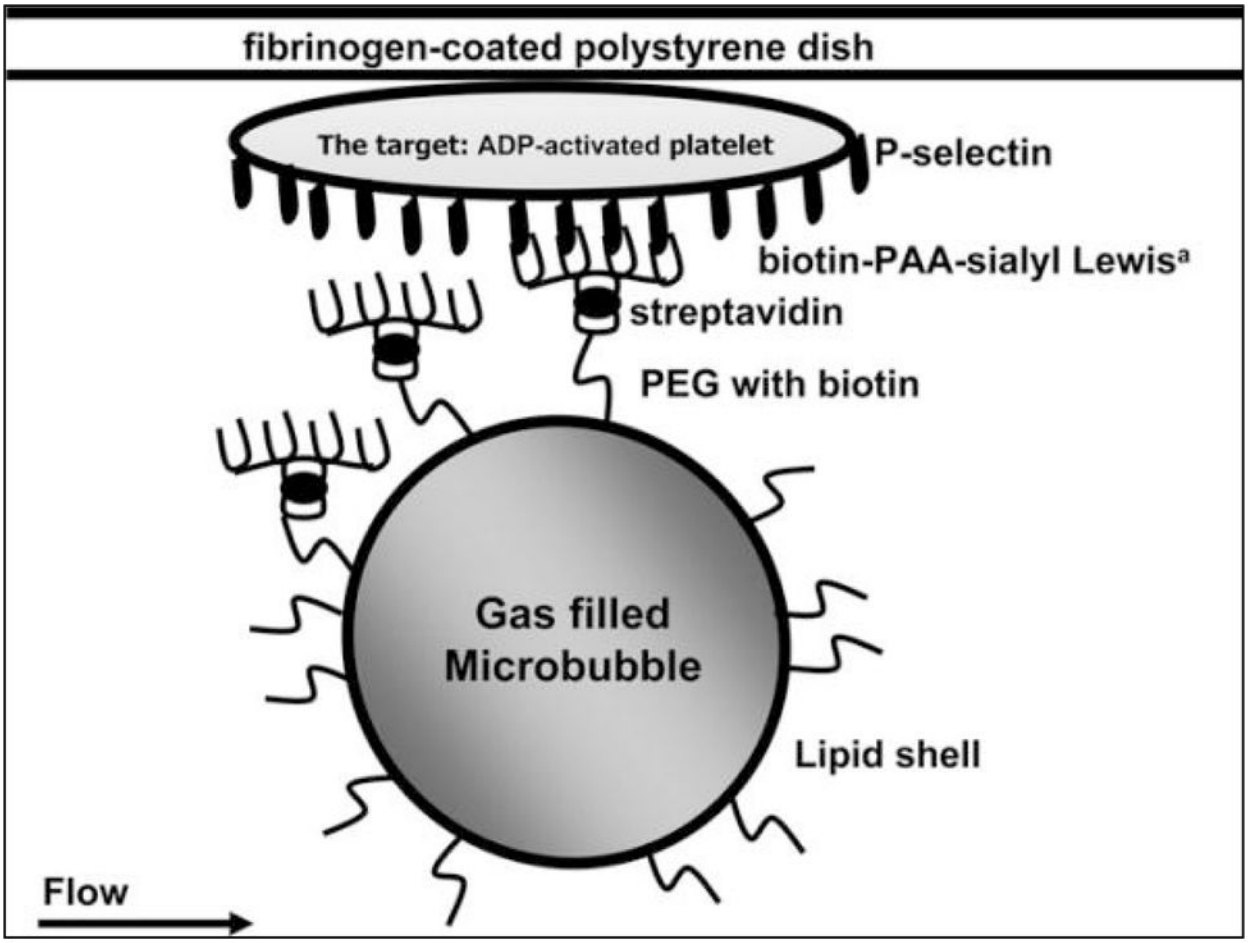

Figure 1.
Targeting scheme of sLe[a]-targeted microbubbles in the flow chamber. MB had biotinylated PEG molecules on their shell and were coupled with biotinylated sialyl Lewis[a] polyacrylamide or a biotinylated control carbohydrate-free polymer. Streptavidin served as a linker.

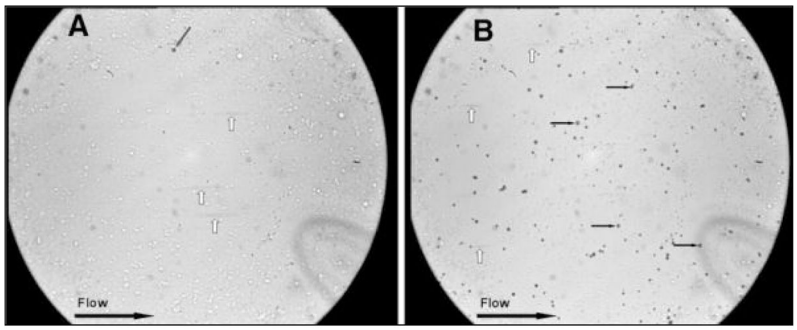

Figure 2.

Flow chamber experiment at 10 dynes/cm^2. Dishes are covered with activated platelets that are expressing P-Selectin on their surface. Field of view is 420 × 350 μm: A: Control MB. The grey arrow indicates a non-specific MB adhesion that happened prior to the high shear flow application. B: sLe^a MB. Black arrows indicate adherent MB which are rolling along the flow path; white arrows indicate MB in the flow which were near the surface and appear as grey stripes.

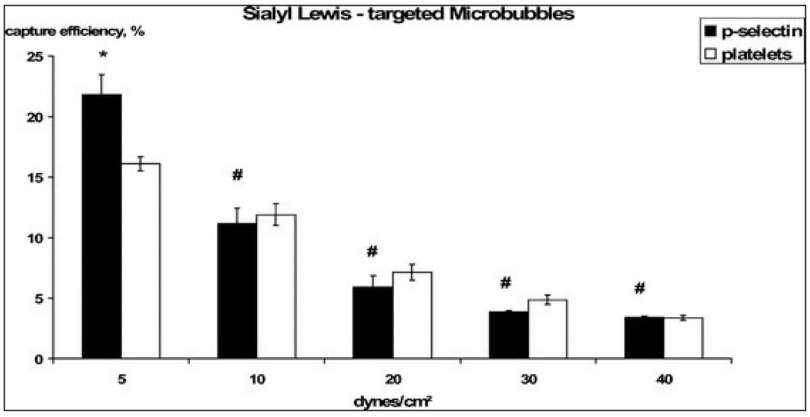

Figure 3.

Mean capture efficiency (± SEM) of sLe^a-MB on recombinant P-selectin and on activated platelets. 35mm culture dishes covered by P-selectin (n=4) or activated platelets (n=5) were perfused by a dispersion of sLe^a MB (5×10^6 MB/ml PBS) at wall shear stress 40, 30, 20, 10, and 5 dynes/cm^2. * indicates a significant difference in capture efficiency at 5 dynes/cm^2, # indicates no significant difference at the other wall shear stress conditions. Capture efficiency was decreasing with increasing shear flow.

Table 1

Mean MB capture efficiency and mean MB flux (± SEM) at each shear flow. The mean capture efficiency (in %) and the mean number of microbubbles in the flow (mean flux) are shown (± SEM) at each wall shear stress in the different groups (n stands for the absolute number of dishes). SLe^a MB that bound at 5 and 10 dynes/cm^2 in group 4 detached immediately after binding (without re-attachment) in contrast to group 1 and 2.

Microbubbles	dynes/cm^2	Capture efficiency %	± SEM	mean flux	± SEM
1. sLe^a on platelets (n=5)	**5**	16.11	0.58	572	55
	10	11.91	0.90	653	79
	20	7.15	0.67	933	126
	30	4.87	0.40	1000	153
	40	3.39	0.20	1129	155
2. sLe^a on recombinant P-selectin (n=4)	**5**	21.84	1.65	841	80
	10	11.16	1.28	941	93
	20	5.89	0.95	1074	92
	30	3.87	0.12	1155	124
	40	3.42	0.10	1417	177
3. sLe^a on fibrinogen (n=3)	**5**	0	0	736	76
	10	0	0	748	21
	20	0	0	885	12
	30	0	0	934	14
	40	0	0	1009	9
4. sLe^a on platelets blocked by anti-P-selectin antibody (n=2)	**5**	0.55	0.12	912	24
	10	0.06	0.06	969	66
	20	0	0	1069	131
	30	0	0	1196	70
	40	0	0	1454	168
5. control on platelets (n=3)	**5**	0	0	878	93
	10	0	0	843	137
	20	0	0	1036	69
	30	0	0	1144	131
	40	0	0	1200	147

Microbubbles	dynes/cm^2	Capture efficiency %	± SEM	mean flux	± SEM
	5	0	0	758	51
	10	0	0	895	86
6. control on recombinant p-selectin (n=3)	**20**	0	0	968	26
	30	0	0	1008	100
	40	0	0	1311	149